Study on Rheological Behavior of Polypropylene/Clay Nanocomposites

Jian Li,[1] Cixing Zhou,[1] Gang Wang,[1] Delu Zhao[2]

[1]*School of Chemistry and Chemical Technology, Shanghai Jiaotong University, Shanghai 200240, China*
[2]*Institute of Chemistry, The Chinese Academy of Science, Beijing 100080, China*

Received 20 May 2002; accepted 15 January 2003

ABSTRACT: Polypropylene/montmorillonite nanocomposites (PPCN) were prepared by melt intercalation with maleic anhydride modified low isotactic polypropylene as the compatibilizer. The linear and nonlinear rheological properties of polypropylene/montmorillonite nanocomposites were studied. The deviation from linear behavior occurred at a strain of 10^0 that was quite less than that for the polymer matrix. The results of dynamic frequency scan showed that the percolation threshold of PPCN was near 3 wt %. Having been subjected to steady preshear, the tactoids could be oriented preferentially in the shear direction, and the percolation network was ruptured. The magnitudes of the stress overshoots observed in the reverse flow experiments were strongly dependent on the rest time, which indicated that the ruptured network could be reorganized even under quiescent conditions. Furthermore, PPCN displayed a strain-scaling stress response to the startup of steady shear. The maxima of the stress overshoots appeared at the stain of 10^0, which was consistent with the strain where the deviation of linear viscoelastic behavior started. It might imply that subjected to the deformation less than 10^0, the network structure could be regard as elastic one. Additionally, the analogous strain-scaling stress response to the startup steady shear elucidated the structural analogy between PPCN and liquid crystal polymer solution. © 2003 Wiley Periodicals, Inc. J Appl Polym Sci 89: 3609–3617, 2003

Key words: polypropylene; montmorillonite; nanocomposites; linear rheological behavior; nonlinear rheological behavior

INTRODUCTION

Polymer-layer silicate nanocomposites (PLSN) have attracted considerable interest stemming from the dramatic enhancements in their physical, thermal, gas barrier, and mechanical properties with the relative low inorganic loading required.[1–12] A large number of polymers with varying degree of polarity and chain rigidity have been used as base polymers for PSLN, including polystyrene,[1] polyamide,[2–4] polyimide,[5] epoxy resin,[6] phenolic resin,[7] polyurethane,[8] poly(butyleneterephthalate),[9] and polypropylene,[10–12] PLSN can be prepared by four different methods: solution intercalation, *in situ* intercalative polymerization, polymer melt intercalation, and exfoliation adsorption. Among them, polymer melt intercalation is the most industrially valuable because of its environmentally benign character, its versatility, and its compatibility with current polymer processing techniques.[13]

Depending on the degree of polymer penetration into the silicate intergallery, there are two idealized types of microstructures in PLSN—namely, intercalated and exfoliated. Intercalated nanocomposites are formed when one or a few molecular layers of the polymer are inserted into the clay gallery with fixed interlayer distance. Exfoliated nanocomposites are formed when the silicate nanolayers are delaminated by the polymer chains and homogeneously dispersed in the polymer matrix. It is believed that the outstanding properties of PLSN come from the structural nature of smectite clay, including large surface area, high aspect ratio, and good interfacial interaction with the polymer matrix, which can be observed especially in the exfoliated nanocomposited.

It has been known that compatibility and optimum interactions between polymer matrix, organic surfactant, and silicate layer surface are crucial to fabricate the intercalated and especially exfoliated nanocomposites by direct melt compounding. However, there are many cases where polymer and organic clay are not compatible enough to form the nanocomposites. To realize the nanoscale dispersion of clay, a third component can be employed as a compatibilizer or intercalating agent to assist the intercalation of polymer chains. Using this technique, Kawasumi et al.[10] first succeeded in preparing polypropylene/montmorillonite (PP/MMT) nanocomposites in presence of a maleic anhydride modified polypropylene oligoemer compatibilizer.

Correspondence to: C. Zhou (cxzhou@mail.sjtu.edu.cn).
Contract grant sponsor: Special Funds for Major State Basic Research Projects; contract grant number: G199906408.

Journal of Applied Polymer Science, Vol. 89, 3609–3617 (2003)

TABLE I
Compositions and Abbreviation of the Prepared Hybrids

	PP (wt %)	LiPP-g-MAH (wt %)	MMT908A (wt %)
PPCN1	96	3	1
PPCN2	92	6	2
PPCN3	88	9	3
PPCN5	80	15	5
PPCN6	76	18	6
PPCN9	64	27	9

In our work, we prepared PP/MMT nanocomposites using maleic anhydride grafted low isotactic homopolypropylene (LiPP-g-MAH) as the compatibilizer in melt processing to fabricate the nanocomposites, where LiPP contains both isotactic and atactic stereosequences. It was found that the compatibilizer based on this new type of polypropylene is effective for the dispersion of clay and the formation of nanocomposites. In this article, a rheological study was conducted on these PP/MMT nanocomposites for two reasons. First, it may provide some useful guidance to overcome the possible difficulties resulting from the large changes in melt viscoelastic properties observed in the nanocomposites. Second, it is believed that the rheometry has been recognized as a powerful tool for investigating the inner microstructures of nanocomposites,[14–17] such as the state of dispersion of clay and, the confinement effect of silicate layers on the motion of polymer chains. In our study, the response of nanocomposites to linear and nonlinear deformation were both investigated, which can provide much important information for understanding the relationship of its rheological behavior and the nature of its microstructures.

EXPERIMENTAL

Materials

PP (grade Montell 5C39F) of M_w = 320,000 was used as the matrix phase. Additive-free low isotactic homopolypropylene elastomer (LiPP) of M_w = 106,000 determined by high-temperature gas permeation chromatography (GPC) (Water-150C, America) was kindly provided by Research Institute of Yanshan Petrochemical Co. LiPP-g-MAH containing 0.31 wt % MAH was prepared in our laboratory by solid phase grafting. The commercial organic MMT (grade 908A) modified with alkyl ammonium was supplied by Huate Co., Zhejiang Province, China.

Preparation

LiPP-g-MAH and MMT-908A was premixed in a Rheomix 600 mixer (Haake Rheocord 900, Germany) at 140°C and 40 rpm for 10 min to fabricate a LiPP-g-MAH/ MMT-908A mixture, where the weight ratio of MMT-908A to LiPP-g-MAH was 1/3. Then the mixture was melt compounded with the PP matrix also in the Rheomix 600 mixer at 200°C and 120 rpm for 10 min to fabricate the PP/clay nanocomposites (PPCN). The compositions of PPCN were listed in Table 1. All the materials were dried at 85°C under vacuum for 24 h before using.

Rheometry

Rheological measurements were carried out in an oscillatory mode on a rheometer (ARES rheometer, Rheometrics Scientific, NJ) equipped with a parallel plate geometry using 25 mm diameter plates at 200°C. All measurements were performed with a 200 FRTN1 transducer with a lower resolution limit of 0.02 g cm. The samples were about 1.5 mm in thickness. In the linear viscoelastic measurements, the small amplitude oscillatory shear was applied, and the dynamic strain scan measurements and the dynamic frequency scan measurements were carried out. In the nonlinear viscoelastic measurements flow reversal studies and startup of steady shear were conducted. For flow reversal experiments, the following deformation history was applied to the sample: First, the sample was sheared for 300 s at shear rate $\dot{\gamma} = 0.1\ s^{-1}$. Next, the flow was stopped, and the sample was kept quiescently for a predetermined time (hereafter referred as the rest time). Finally, the sample experienced a shear in the reverse direction for 300 s at shear rate $\dot{\gamma} = 0.1\ s^{-1}$. The shear stress was monitored during this period. In steady shear measurements, the transient stress response to the startup of the shear of various shear rates was recorded.

Microstructure characterization

The degree of swelling and the interlayer distance of the clay in PPCN were determined by wide angle X-ray

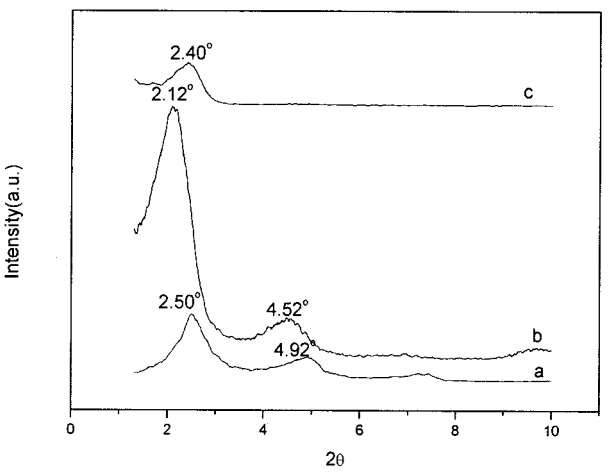

Figure 1 WAXD patterns for clay and PPCN samples: (a) 908A, (b) PPCN6, and (c) PPCN9.

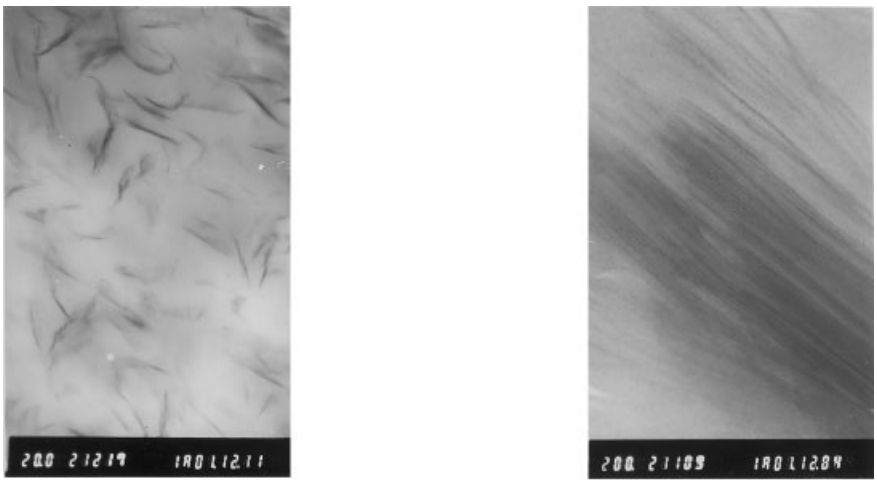

(a) (b)

Figure 2 EM images of PPCN6 at two different magnifications of (a) 20,000 and (b) 200,000.

diffraction (WAXD). The X-ray diffraction experiments were performed using Rigaku Dmax-rC diffractometer with CuK_α radiation of wavelength 1.54 Å and a rotating anode generator operated at 40 kV and 100 mA. The scanning rate was 2° min from 1.5° to 10°. The PPCN samples for WAXD measurements were prepared in films by compression molding at 200°C and 5 MPa. The transmission electron micrographs were taken from 80 to 100 nm thick, microtomed sections of the PPCN samples using a transmission electron microscope (Hitachi H-860, Japan) with 100 kV accelerating voltage.

RESULTS AND DISCUSSION

Phase morphology in PPCN

Figure 1 shows the WAXD results of the organic clay MMT-908A and PPCN containing various clay loadings. The original peaks of MMT-908A remain in PPCN6 and PPCN9, but shift to lower angles. It indicates that the ordered multilayer structure of the clay in PPCN6 and PPCN9 still remained, but the intergallery of silicate layers expanded due to the intercalation of LiPP-g-MAH. The interlayer distance of the clay for PPCN6 and PPCN9, in comparison with that of the original clay, increased from 35.4 to 41.6 and 36.8 Å respectively. It is notable that the WAXD pattern of PPCN9 shows that the basal reflection of 908A in PPCN9 decreased in intensity, although it contained the largest clay loading. This means that some silicate layers may be exfoliated from the stacks. Since the melt intercalation process is controlled by the mass transport of polymer chain into primary particles of clay, tactoids near the edge may accessible to the polymer chain.[13] Thus it can be inferred that that

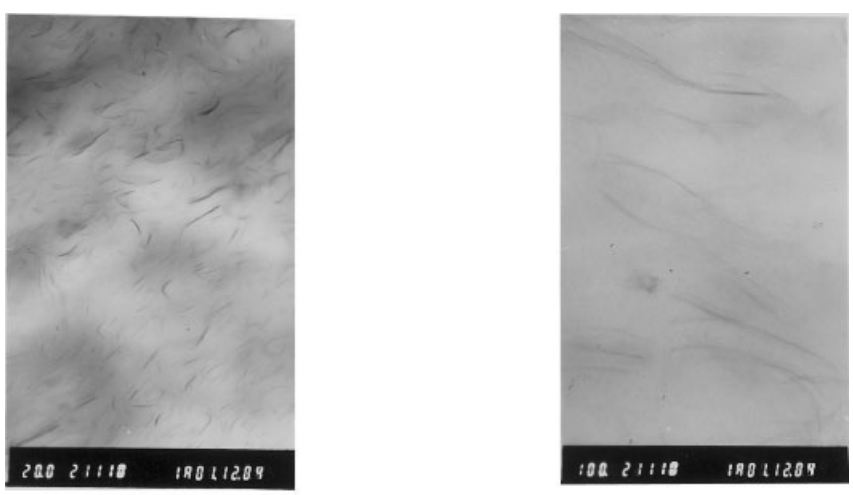

(a) (b)

Figure 3 EM images of PPCN9 at two different magnifications of (a) 20,000 and (b) 100,000.

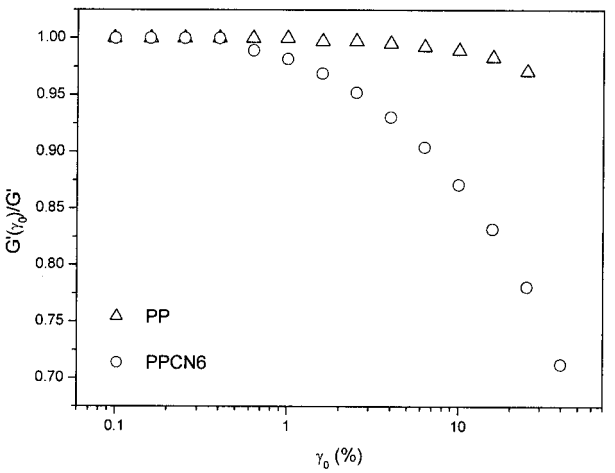

Figure 4 Strain dependence of the normalized storage modulus of PP and PPCN6.

silicate layers at the end of the silicate stacks may be relative easy to be exfoliated. The exfoliation to silicate layer on the margin of the particles may even come before the intercalation to those layers near the particle center like in PPCN9 since a large amount of LiPP-g-MAH was added in. It means that the virgin organic clay, intercalated tactoids, and exfoliated layers may coexist in PPCN9 forming a complicate structure.

To further confirm the dispersion states of the clay in the matrix, transmission electron microscopy (TEM) studies at varying magnifications were carried out. Figure 2(a) presents the TEM image of PPCN6 at a magnification of 20,000, which shows the tactoids composed of several tens of silicate layers are disperses in the matrix. Figure 2(b) shows the distinct fine intercalated structure composed of alternating polymer layers (bright lines in the image) and silicate ones (dark lines). Figure 3(a) shows the TEM image of PPCN9 at a magnification of 20,000. As can be seen, the thickness of 908A in PPCN9 is noticeably decreased in comparison with that in PPCN6. Additionally, the TEM image at a magnification of 100,000 was also taken. As shown in Figure 3(b), individual silicate layers of about 1 nm thickness and thin silicate sheet composed of several layers can be seen, which does further support the result of the WAXD measurement. Thus the TEM images are quite in agreement with WAXD measurements.

Linear viscoelastic properties

In order to determine the region of linear viscoelastic behavior, the dynamic strain scan was conducted. Figure 4 shows the development of the normalized storage modulus for PPCN6 with the strain. It can be known that the region of linear viscoelastic behavior changed greatly in the presence of the intercalated clay. The deviation from linear behavior for PPCN6 occurred at the strain of about 1%, which was much less than for pure PP. Therefore, the following dynamic frequency scan measurements were conducted at the strain of 0.1%.

The storage modulus (G') data and loss modulus (G'') data resulting from the dynamic frequency scan measurements for PPCN with various clay loading are compared in Figure 5(a) and Figure 5(b), respectively. Figure 5(a) shows the effect of clay loading on G' of PPCN, in which the magnitude of G' monotonically increased with clay loading at low frequencies. The same trend is also observed in Figure 5(b) for the G'' curves. It is believed that the degree of dependence of low-frequency G' on the frequency, ω, reflects sensitively the effect of clay on the viscoelatic properties of the nanocomposites. Therefore, to explore the influ-

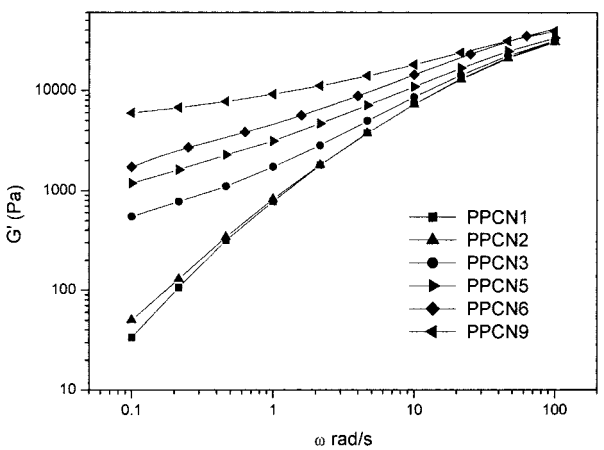

(a)

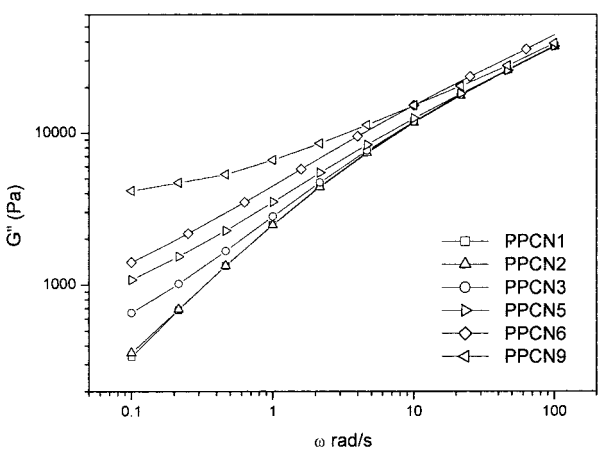

(b)

Figure 5 Comparison of dynamic shear modulus of PPCN (a) storage modulus and, (b) loss modulus.

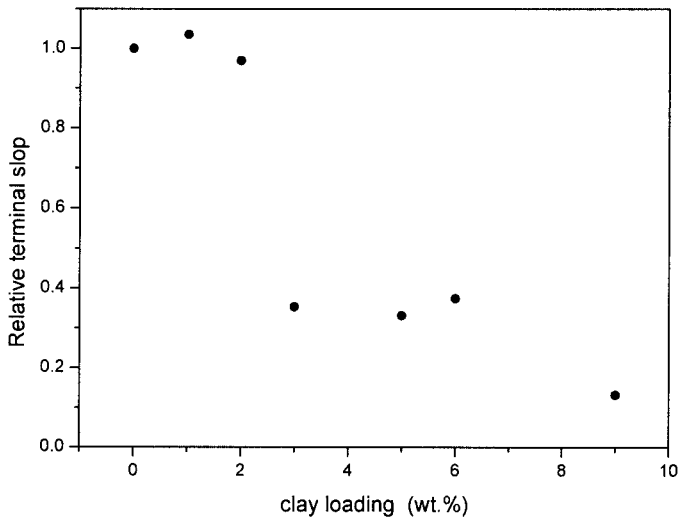

(a)

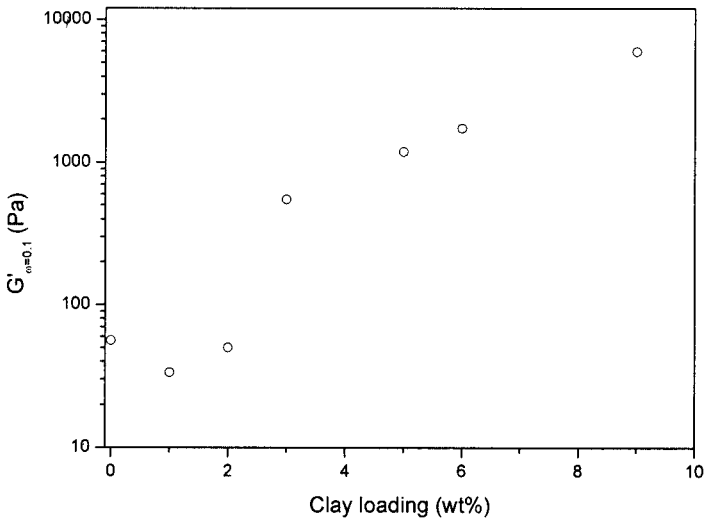

(b)

Figure 6 (a) The dependence of relative terminal slope on clay loading. (b) The dependence of the low-frequency storage modulus measured at $\omega = 0.1$ rad/s on clay loading.

ence of clay on the rheological behavior of the nanocomposites, the dependence of G' on the frequency, ω, at low frequencies was studied. Compared in Figure 6(a) are the relative terminal slopes of G' vs ω for PPCN (determined by the ratio of terminal slope for pure polypropylene matrix to those for PPCN). The dependence of G' and ω for PPCN1 and PPCN2 are quite similar to that of the pure polypropylene matrix, which exhibits a near terminal behavior ($G' \sim \omega^2$). With clay loading exceeding 3 wt %, the dependencies of G' of PPCN on ω decrease sharply in the terminal zone, and as can be seen in Figure 5(a), the G' curves exhibit a plateau at the low frequencies. It indicates that the viscoelastic properties are still dominated by the polymer matrix when the clay loading is below 3 wt %, and PPCN may experience a transition from

liquid-like behavior to solid-like one with the clay loading up to 3 wt %. The solid-like viscoelastic response results from the formation of percolation network as reported by other workers.[17,18] As a result, the percolation threshold for PPCN is approximately 3 wt %. It can be found that the percolation limit for PPCN is much lower than that for traditional composites, which results from the high geometric anisotropy and specific surface area of the plate-like silicate tactoids.[19] To further study the clay effect of clay on the rhoelogical behavior, the dependence of the enhancement in low-frequency G' on the clay loading is also probed. Generally, the contribution of intercalated clay to G' of the nanocomposites (G'_{nano}) can be analyzed in terms of two effects: the confinement effect (G'_{con}) and the interparticle interactions (G'_{inter}), which results in the enhancement of low-frequency G' in comparison with the polymer matrix (G'_{matrix}), i.e.,

$$G'_{nano} = G'_{matrix} + G'_{confine} + G'_{inter} \quad (1)$$

Here $G'_{confine}$ arises from the confinement of silicate layers with an interlayer distance smaller than or of the same order of the size of the chain coils that may lead to the alternation of the relaxing dynamic of the intercalated polymers. G'_{inter} comes from frictional interactions between the tactoids. These interactions can sharply increase when the clay loading is above a percolation threshold, which may lead to the significant enhancement of low-frequency G'. Figure 6(b) shows the low-frequency G' measured at frequency of 0.1 rad/s as a function of the clay loading. Compared with the PP matrix, the low-frequency G' of PPCN1 and PPCN2 does not increase distinctly, and G' of PPCN1 is even a bit less than that of the matrix because of the plasticizing effect of LiPP-g-MAH with lower molecular weight. Therefore, both $G'_{confine}$ and G'_{inter} are quite small in PPCN1 and PPCN2. The contribution of G'_{inter} is very small because clay loading is below the percolation limit. We can also see the contributions of $G'_{confine}$ for PPCN1 and PPCN2 are also marginal, which is consistent with their near linear viscoelastic terminal behavior at low frequencies. However, it does not imply that the relaxation of the intercalated polymer or that near the surface of the layers is unaffected. Perhaps our experiments here are incapable of probing the changes of relaxation of the intercalated or absorbed chains because their relaxation processes may be much slower than the time scale of the experiments. The low-frequency G' enhanced sharply when the clay loading is up to 3 wt %, which obviously resulted from the physical jamming. G'_{nano} may be dominated by G'_{inter} because the contribution of G'_{inter} is much larger than those of G'_{matrix} and $G'_{confine}$ at the low frequencies. On the other hand, if the percolation network is destroyed, the viscoelastic behavior may change greatly. Figure 7 shows the effect of steady preshear on the rheological behavior. The dynamic modulus of presheared PPCN6 decreased remarkably and its low-frequency dependence enhanced, which indicates that the viscoelastic behavior changed from solid-like to liquid-like one after the steady preshear. From this result, it can be expected that the platelet-like tactoids were oriented preferentially in the shear direction and did not form a percolation network structure under present loading.

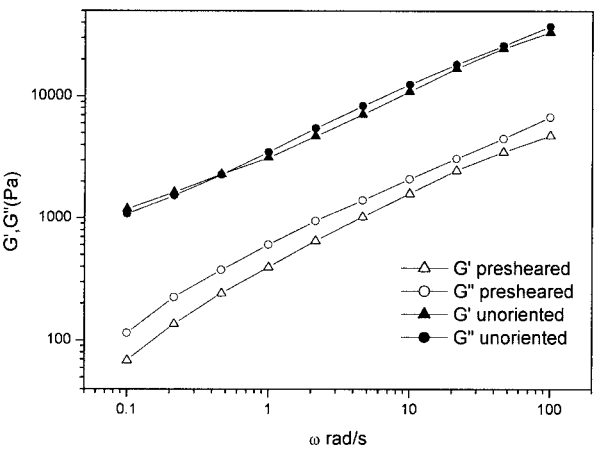

Figure 7 The effect of steady preshear on the linear rheological behavior.

Nonlinear viscoelastic properties

Since the region of linear viscoelastic behavior is very sensitive to the presence of clay that results in the formation of percolation network, the study on the linear viscoelastic properties of PPCN is limited in a quite narrow strain region, which impedes our attempt to further investigate the nature of the percolation structure. The nonlinear rheological measurements, however, may facilitate the insight into the microstructure of PPCN.

Figure 8 shows the normalized transient stress response of PPCN6 in the reversal flow experiments at 200°C. It is obvious that the magnitudes of the stress overshoot have distinct dependence on the rest time. When the reverse direction shear was immediately imposed to the sample without rest, the overshoot was too weak to be detected by the instrument. With the increase of the rest time, the magnitude of the overshoot increased monotonously. The strong dependence of the magnitude of the stress overshoot on the rest time is indicative of the structural evolution in the sample during the quiescent period. Initially, the steady shear for 300 s resulted in the rupture of percolation network due to the preferential orientation of the tactoids in the shear direction, which also was observed in the previous experiment. Then the ruptured network could be reorganized even under the

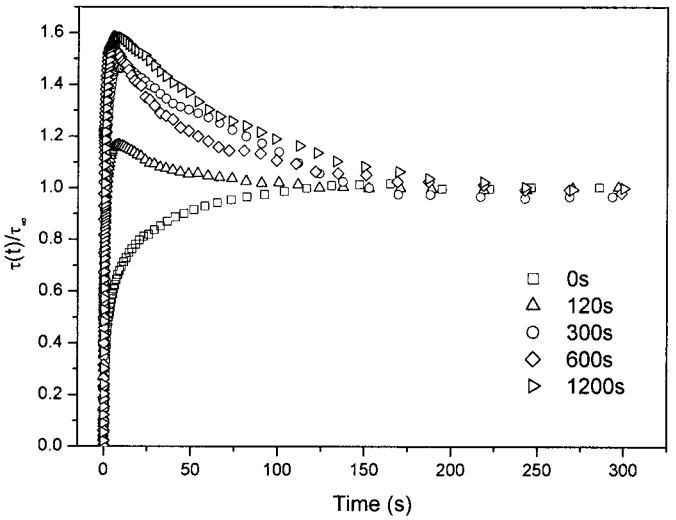

Figure 8 The stress response to the startup of steady shear in the reverse flow measurement.

quiescent condition, which was indicated by the appearance of the stress overshoots. Perhaps Brownian motion may be one of the possible mechanisms for the reorganization. Therefore the rotary relaxation of Brownian motion is introduced here. Assuming that the tactoids dispersed in the polymer matrix is circular plate-like in shape, the rotary diffusivity, D_{r0}, is obtained as follow[20]:

$$D_{r0} = \frac{3k_BT}{4\eta_m d^3} \tag{1}$$

We assume that a tactoid will rotate for a quarter period, $1/2 \cdot \pi$, to complete rotational relaxation. Therefore the rotational relaxation time, t_0, due to Brownian motion is approximately

$$t_D \approx \frac{(\frac{1}{2}\pi)^2}{D_{r0}} = \frac{\pi^2\eta_m d^3}{3k_BT} \tag{2}$$

where η_m is the viscosity of the matrix, d the diameter of the tactoid, k_B the Boltzmann constant, and T the temperature. Therefore, considering the polypropylene matrix with η_n of about 4000 Pa s, t_D for the tactoid with d of 500 nm is about 2.7×10^5, which is larger than the time scale in our experiments by 3 orders. From this result, it is clear that Brownian motion is not the major force for the reorganization of the network. The drive force for the reorganization of the network may come from the strong interaction between the tactoids themselves.[15] It needs to be pointed out that the overshoot in the reverse direction flow was absent regardless of the rest time when the clay loading is less than 3 wt %, which further confirms that the overshoot is an indication of the network structure.

In order to further investigate the nature of their microstructures, the transient stress responses of PPCN to the start-up of steady shear flows with various shear rates were studied at the temperature of 200°C. Figure 9 shows the results for PPCN6. As can be seen, the magnitudes of the stress overshoot seem to be strongly dependent on both the time and the shear rates applied to the sample. However, if the transient stress is plotted against strain $\gamma = \dot{\gamma}t$ as shown in Figure 10, we can see that the overshoots scale with the strain. This result is quite consistent with that of Solomon et al.'s work.[15] Additionally, the maxima of the stress overshoot all approximately appeared at γ of about 10^0. As known from the dynamic strain scan measurements, the deviation from the linear viscoelastic behavior also happened at the strain of about 10^0. This coincidence may imply that the network structure is sensitive to the strain, and could be regarded as elastic one to the deformation less than 10^0. In the elastic deformation region, the stress scales with the strain, and the structure is not ruptured or the recovery of the deformation is quick enough. With the stain greater than 10^0, the network structure may be ruptured, and the deformation become unrecoverable. Furthermore, from some study on the nonlinear viscoelastic properties on liquid crystalline polymer solutions (LCPS), the analogous strain-scaling stress response to the steady shear was also observed,[20], which indicates the structural analogy between PPCN and LCPS. According to Valeriy et al.'s, work[21] on the phase diagrams of polymer/clay composites, clay sheets may experience orientational ordering and can form liquid crystalline phases (such as nematic, smectic, columnar, or plastic solid) because of their high geometric anisotropy and aspect ratio. Therefore our study on the nonlinear viscoelatic of PPCN indicates

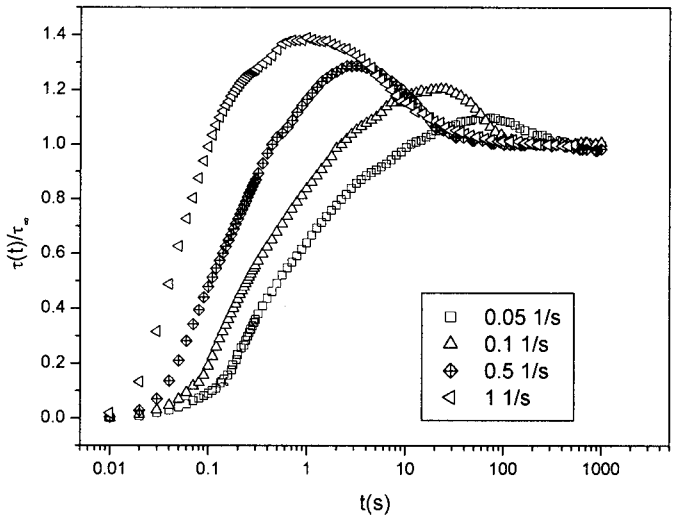

Figure 9 Transient shear–stress response as a function of time to the startup of steady shear flows at different shear rates.

indirectly that the liquid crystal-like structures may be the nature of the polymer/clay nanocomposites.

CONCLUSIONS

The silicate crystallites or tactoids have a great effect on the rheological behaviors of the PPCN. In the linear viscoelastic measurements, PPCN display a strain-sensitive linear behavior region much narrower than that of the polymer matrix. When the clay loadings is up to 3 wt %, the percolation network may form, which leads to the remarkable enhancement of the low-frequency G' and the transition from a liquid-like behavior to solid-like one, which indicates that the percolation threshold of PPCN is near 3 wt %. Having been subjected to steady preshear, the low-frequency G' decreases sharply and its frequency dependence increases distinctly, which indicates that the tactoids may be oriented preferentially in the shear direction, and the percolation network was ruptured. From the results of the reverse flow experiments that the magnitudes of the stress overshoots are strongly dependent on the rest time this shows that the ruptured network could be reorganized even under quiescent conditions. Additionally, it shows that the driving force for the reorganization is not Brownian motion. PPCN display a strain-scaling stress response to the startup of steady shear. The maxima of the overshoots in stress appear at the strain of 10^0, which is consistent with the strain where the deviation of linear viscoelasticity starts. This may imply that the network structure could be regarded as an elastic one subjected to the deformation less than 10^0. Furthermore, the analogous strain-scaling stress response to the startup steady shear may indicate the structural analogy between PPCN and LCPS.

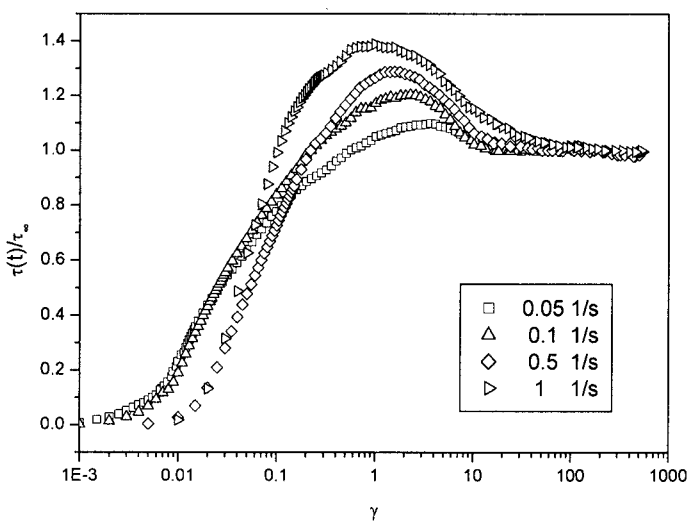

Figure 10 Transient shear stress response as a function of strain to the startup of steady shear flows at different shear rates.

References

1. Vaia, R. A.; Jandt, K. D.; Kramer, E. J.; Giannelis, E. P.; Chem Mater 1996, 8, 2628.
2. Kojima, Y.; Usuki, A. M.; Kawasumi, A.; Okada, T.; Kurauchi, Kamigaito, O.; J Polym Sci, Part A: Polym Chem 1993, 31, 983.
3. Wu, Z. G.; Zhou, C. X.; Qi, R. R.; Zhang, H. B. J Appl Polym Sci 2002, 83, 2403.
4. Wu, Z. G.; Zhou, C. X.; Polym Test, accepted.
5. Tyan, H. L.; Liu, Y. C.; Wei, K. H. Polymer 1999, 40, 4877.
6. Lan, T.; Kaviratna, P. D.; Pinnavaia, T. J. J Phys Chem Solids 1996, 57, 6.
7. Wu, Z. G.; Zhou, C. X.; Qi, R. R. Polym. Polym. Compos, in press.
8. Ma, J.; Zhang, S.; Qi, Z. N.; J Appl Polym Sci 2001, 82, 1444.
9. Li, X. C.; Kang, T.; Cho, W. J.; Lee, J. K.; Ha, C. S. Macromol Rapid Commun 2001, 21, 1040.
10. Kawasumi, M.; Hasegawa, N.; Kato, M.; Usuki, A.; Okada, A. Macromolecules 1997, 30, 6333.
11. Usuki, A.; Kato, M.; Okada, A.; Kurauchi, T. J. Appl Polym Sci 1997, 63, 37.
12. Hasegawa, N.; Okamoto, H.; Kato, A.; Uauki, M. J Appl. Polym Sci 2000, 78, 1918.
13. Vaia, R. A.; Janndt, D. K.; Kramer, E. J.; Giannelis, E. P. Macromolecules 1995, 28, 8080.
14. Lim, Y. T.; Park, O. O.; Rheol. Acta 2001, 40, 220.
15. Solomon, M. J.; Almusallam, A. S.; Seefeldt, K. F.; Somwangthanaroj, A.; Varadan, P. Macromolecules 2001, 34, 1864.
16. Krishnamoorti, R.; Giannelis, E. P. Macromolecules 1997, 30, 4097.
17. Galgali, G.; Ramesh, C.; Lele, A. Macromolecules 2001, 34, 852.
18. Ren, J.; Silva, A. S.; Krishnamoorti, R. Macromolecules 2000, 33, 3739.
19. Bicerano, J.; Douglas, J. F.; Brune, D. A. J Polym Sci—Rev Macromol Chem Phys 1999, 34, 561.
20. Larson, R. G. The Structure and Rheology of Complex Fluids; Oxford University Press: New York, 1999.
21. Valeriy, V.; Ginzburg, C. S.; Balazs, A. C. Macromolecules 2000, 33, 1089.